Journal of Research in Environmental and Earth Sciences

Volume 11 ~ Issue 11 (November 2025) pp: 69-76

ISSN(Online) :2348-2532 www.questjournals.org



Research Paper

Spatial Variability of The Storm-Time Geo-Electric Disturbances Across the West African Equatorial Belt

Akanigwo C.D

¹Department of Physics/Industrial Physics, Nnamdi Azikiwe University, P.M.B. 5025, Awka, Anambra State, Nigeria.

Corresponding Author: Akanigwo Chidimma Dorathy

ABSTRACT

This study investigates the spatial variability of the storm-time geo-electric disturbances across West Africa'n equatorial belt with the data obtained from nine Observatories in Africa. Dst. Index values of < -100nT were classified as stormy days. The analysis began with the examination of geo-electric field component charts from the available data, corresponding to the stormy days, derived from the telluric measurements collected along the meridional chain in 1992 and 1993. The results show that the geo-electric field response to geomagnetic storms is dependent on location, influenced by local ground conductive materials and regional conditions.

KEYWORDS: Geo-electric field, storm-time, Earth's magnetic field, Variation, Dip Equator

Received 05 Nov., 2025; Revised 14 Nov., 2025; Accepted 16 Nov., 2025 © The author(s) 2025. Published with open access at www.questjournas.org

I. Introduction

A geomagnetic storm is a major disturbance of Earth's magnetosphere that occurs when there is a very efficient exchange of energy from the solar wind into the space environment surrounding Earth. Geomagnetic storms are also disturbances of the Earth's magnetic field resulting from perturbations in the interplanetary magnetic field

(IMF)" [12].

In space, a ring of westward current around Earth produces magnetic disturbances on the ground. A measure of this current, the disturbance storm time (Dst) index, has been used historically to characterize the size of a geomagnetic storm. A standard geomagnetic storm usually has 3 phases: the initial phase, main phase and recovery phase.

The initial phase is usually caused by an enhancement of the solar wind behind shock

wave. The main phase is characterized by the depression of the Horizontal (H) component of the Earth's magnetic field, and is followed by the recovery phase which is characterized by the slow and quiet return of the H component of the magnetic field to its pre-storm level [2]. The degree of depression of the H component of the geomagnetic field during geomagnetic storms varies, depending on the magnetic local time. In this case, the maximum depression of the H component of geomagnetic field strength is seen on the night to dusk side, while the minimum depression of the H component is seen on the day to dawn side. This is as a result of the asymmetrical flow of the ring current. Generally, the recovery phase of any storm takes longer than the initial and main phases [5].

Geomagnetic field on the other hand, is the observed magnetic field on Earth caused by the interference of magnetic field produced either by a magnetic dynamo in the Earth's liquid or by the electric currents in the ionosphere and magnetosphere [1]. The time variations are divided into long and short term variations. The long term (secular) variations come from the dynamics of Earth's interior while short term variations have

an external origin [8]. The short term variations last from within seconds up to a year. They are often intense and are mainly produced by currents in the magnetosphere and ionosphere [11]; [8] Studying the storm time variations of the Earth's magnetic field during the recovery phase of a geomagnetic storm is important in improving space weather impact predictions and technological and infrastructure protection in the low and mid latitude regions. Storm time variations of the Earth's Magnetic field are determined by examining the fluctuations of the magnetic field during geomagnetic storm occurrences. During some days, the Earth's magnetic field

undergoes smooth and regular variations while on some other days they undergo irregular changes [3]. Recently, researchers have investigated the variation in the geo-electric field. In view of its significance regarding the impact of space weather on technological systems, have not been thoroughly examined, particularly in the African region, in contrast to the geomagnetic field. While some research has been conducted, including studies by [11], [4], [7], and [6], these investigations were focused on dip equatorial latitudes. The authors of these studies observed that there are daily fluctuations in the geo-electric field. Recognizing the gap in geo-electric field research within the African region, a network of 10 electromagnetic stations was established along the African longitudes during the French involvement in the International Equatorial Electrojet Year experiment (IEEY). The electric field measurements taken during that experiment will be utilized in this study to explore the effects of geomagnetic storms on the variation of the geo-electric field at the dip equatorial latitude of West Africa.

II. MATERIALS AND METHODS

The dataset utilized in this analysis comprises hourly mean values of the North-South Component (Ex) and the East-West Component (Ey) of the geo-electric field, sourced from ten geomagnetic and geoelectrical stations established during the IEEY in Africa. These stations are situated between Ivory Coast to the South and Mali to the North. The stations include Korhogo (KOR), Koutiala (KOU), Lamto (LAM), Mopti (MOP), Nielle (NIE), San (SAN), Sikasso (SIK), Tiebissou (TIE), and Tombouctou (TOM) (refer to Table 1).

Table 1. Geographic coordinates of the magnetic stations installed along the meridian 5 □ W in West Africa during the International Equatorial Electrojet Year.

Stations	Stations Code	Latitude (°N)	Longitude (°W)	Dip Latitude (°N)
Tombouctou	TOM	16.73	3.00	6.76
Mopti	MOP	14.51	4.09	4.02
San	SAN	13.24	4.88	2.45
Koutiala	KOU	12.36	5.45	1.38
Sikasso	SIK	11.34	5.71	0.12
Nielle	NIE	10.20	5.64	-1.30
Korhogo	KOR	9.34	5.43	-2.38
Katiola	KAT	8.18	5.043	-3.85
Tiebissou	TIE	7.22	5.243	-5.04
Lamto	LAM	6.23	5.02	-6.30

The analysis started with checking for the stormy days using 1hour Dst index values obtained from the WDC site. The storm was characterized following [3] nomenclature. Table 2 shows the characterization.

Table 2 Nomenclature often used in classification of geomagnetic Storms (Gonzalez et al., 1994)

Storm	Minimum	Minimum	Time
Classification	Dst (nT)	Bz (nT)	Time
Weak	-30	-3	1h
Moderate	-50	-5	2h
Intense	-100	-10	3h
Super-intense	-500	-50	>3h
Extreme	< -500	<-50	<3h

The storms considered are those with Dst. magnitude of \leq -100nT. These sets of storms so selected represent intense (moderate) storms which are seen to have three phases: initial, main and recovery phases. It began with a broad search of these phases. Here we defined the main phase as the maximum (least intense) Dst within the 24hrs preceding the peak. The end of the recovery phase was determined by locating the Maximum Dst within 96hrs after the peak. The Dst index profiles of the stormy days depicting a day before the storm, stormy day and the day after the storm were plotted. From the available data, the geomagnetic and geo-electric fields (Ex and Ey) profiles of those stormy days were also plotted across the ten stations and the variations of these storms were examined.

III. RESULTS AND DISCUSSION

Four geomagnetic storms have been studied within 1992 and 1993. The four geomagnetic storms considered are the geomagnetic storm of 29th December 1992, 9th March 1993 and 11th March 1993.

This research examines spatial Variability of the storm-time Geo-Electric disturbances across West African Equatorial belt. It focuses primarily on four storms: February 17, 1993; March 9, 1993; March 11, 1993; and April 5, 1993. The Dst Index profiles of each storm were analyzed to determine the phases of storm development, including the Sudden Storm Commencement (SSC), the main storm phase, and the recovery phase.

The figures in 1, 2, 3, and 4 depict the Dst profiles of February 17, 1993, March 9, 1993, March 11, 1993, and April 5, 1993 storms, respectively.

February 17, 1993 Storm

Examining the Dst Index profile for February 17, 1993, a sharp increase around 03:00 LT was noticed, indicating the SSC. The index reached a minimum of -110 nT at 16:00 LT, which marks the main storm phase. Data from four stations—KOU, NIE, LAM, and MOP—were analyzed. The geo-electric field responses at these stations showed variability, with KOU exhibiting the strongest response.

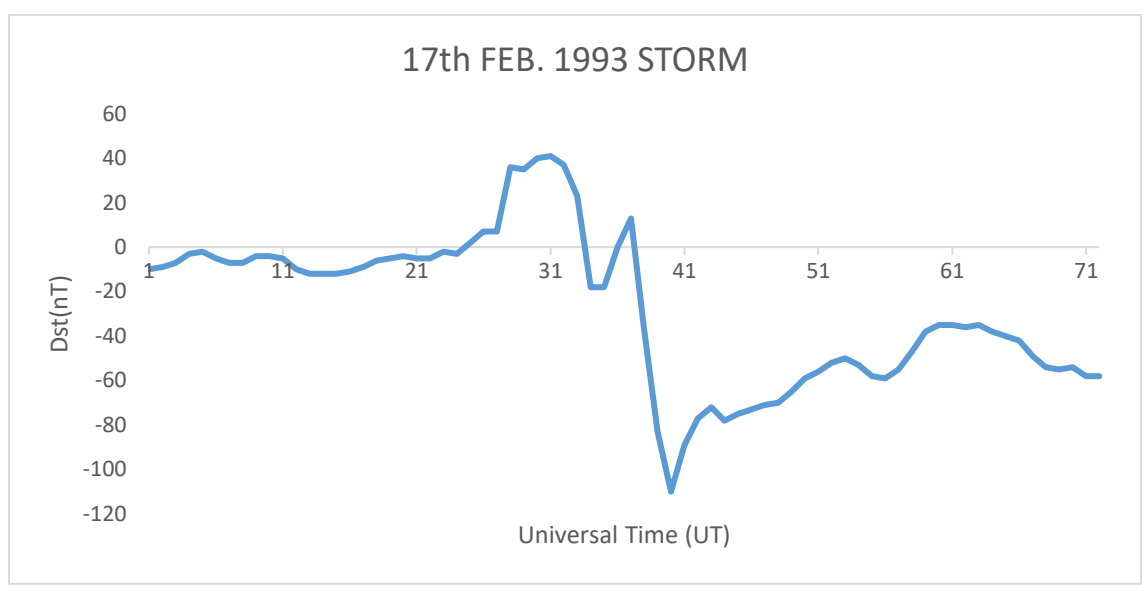


Figure 1: Dst Index Profile for February 17, 1993.

March 9, 1993 Storm

For March 9, 1993 Dst Index profile, a sudden increase in the Dst Index was observed at 11:00 LT. It showed the SSC with a value of 16 nT. The index reached a minimum of -137 nT around 31:00 UT before entering the recovery phase. This behavior aligns with [13] findings, which suggest that a sustained interval of magnetic field enhancement results in increased geomagnetic activity, followed by a recovery phase when the magnetic field weakens.

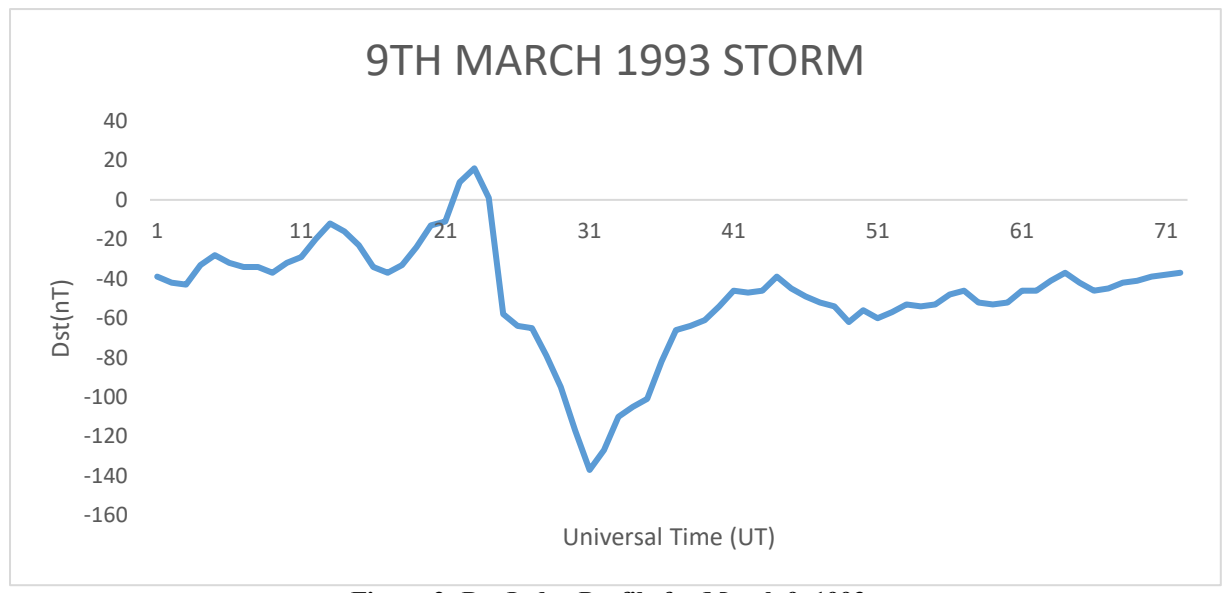


Figure 2: Dst Index Profile for March 9, 1993.

March 11, 1993 Storm

The March 11, 1993 storm upon examination showed an SSC at -38 nT around 01:00 UT. The Dst Index fell to a minimum of -120 nT at 07:00 LT, with the recovery phase beginning at 12:03 UT with a Dst Index of -61 nT. This storm demonstrated a typical storm development cycle, including a clear recovery phase.

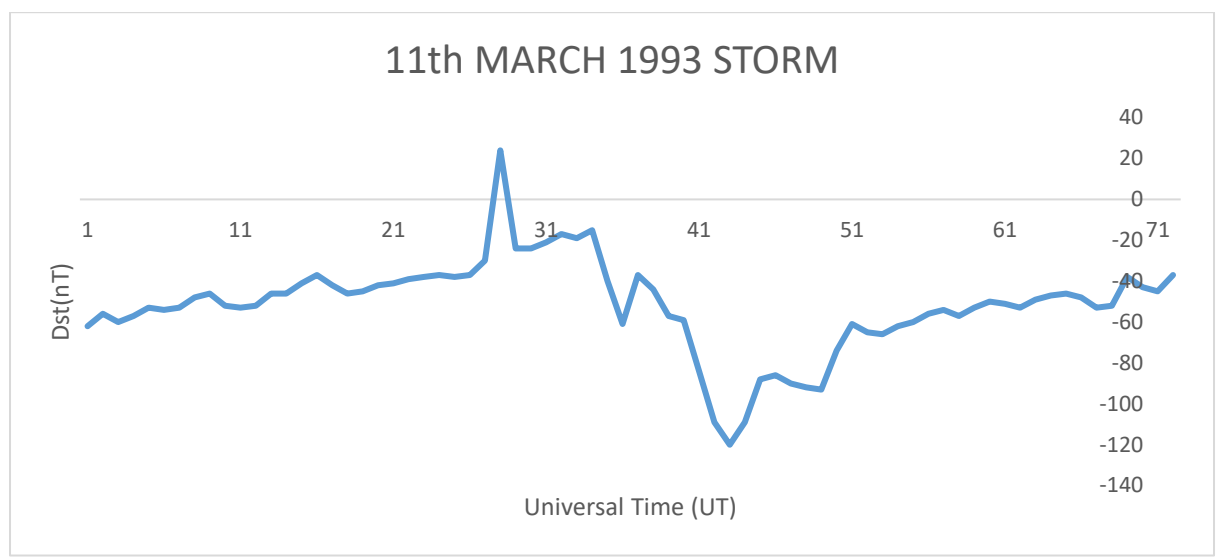


Figure 3: Dst Index Profile for March 11, 1993.

April 5, 1993 Storm

On April 5, 1993 storm, there is no observable SSC before the storm. The Dst Index dropped to -165 nT at 01:00 LT, indicating a significant storm phase. The recovery phase began around 03:00 LT with a Dst Index of -137 nT.

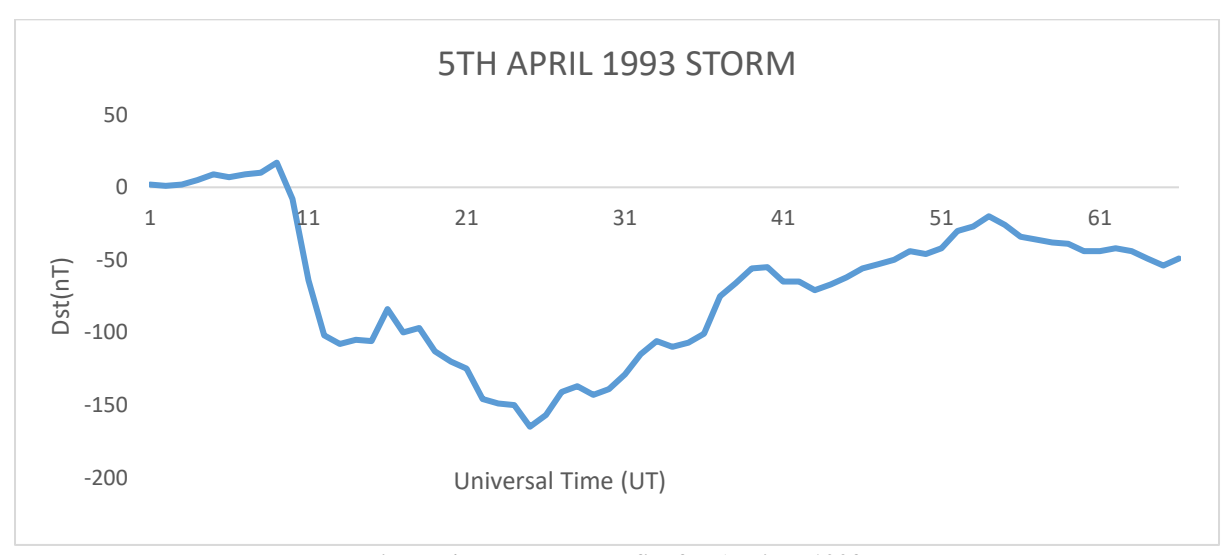


Figure 4: Dst Index Profile for April 5, 1993.

3.1. GEO-ELECTRIC FIELD RESPONSE

The geo-electric field responses during the storm-time of February 17, 1993; March 9, 1993; March 11, 1993; and April 5, 1993 were examined as follows: February 17, 1993

3.2. The geo-electric field responses to the February 17 storm showed varying magnitudes across stations are shown in figure 5. below. The SSC was observed at 13:00 UT with the following values:

KOU: Ex = 209.4 mV/km, Ey = 265.9 mV/km LAM: Ex = 411.8 mV/km, Ey = 432.7 mV/km MOP: Ex = 207.7 mV/km, Ey = 221.2 mV/km NIE: Ex = 87.5 mV/km, Ey = 105.2 mV/km SIK: Ex = 300.6 mV/km, Ey = 320.3 mV/km

During the main storm phase at 16:00 UT: KOU: Ex = 218.9 mV/km, Ey = 290.5 mV/km LAM: Ex = 300.8 mV/km, Ey = 386.3 mV/km MOP: Ex = 212.5 mV/km, Ey = 219.5 mV/km NIE: Ex = 87.5 mV/km, Ey = 95.9 mV/km

SIK: Ex = 307.2 mV/km, Ey = 313.4 mV/km

For the recovery phase: KOU: Ex = 229.4 mV/km, Ey = 298.4 mV/km- LAM: Ex = 305.8 mV/km, Ey = 401.7 mV/km

MOP: Ex = 213.3 mV/km, Ey = 213.2 mV/km NIE: Ex = 92.2 mV/km, Ey = 96.3 mV/km

The variations in geo-electric field responses showed no clear latitudinal pattern, with KOU, a dip-latitudinal station, demonstrating a stronger response compared to MOP, while NIE exhibited minimal response.

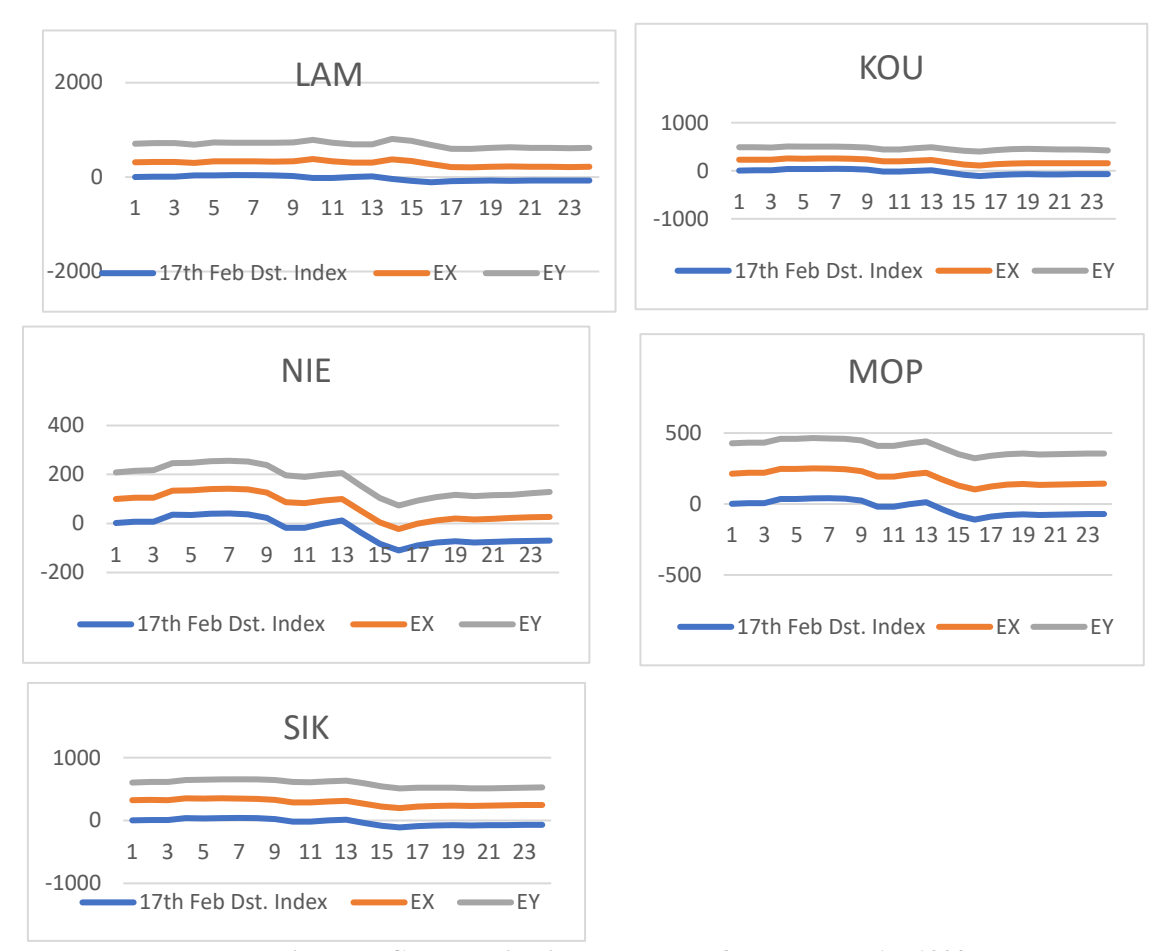


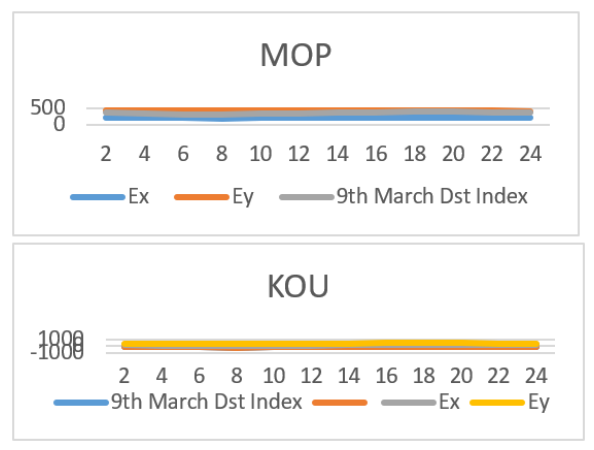
Figure 5: Geo-electric Field Responses for February 17, 1993.

March 9, 1993

Figure 6 shows the response of geo-electric field to the storm that occurred on the 9th March 1993 around 07:00LT across the stations. For this storm, no SSC was detected. The main storm phase, marked by a Dst Index of -137 nT at 08:00 UT, and the recovery phase were analyzed:

- MOP: Ex = 210.2 mV/km, Ey = 217.5 mV/km (main phase), Ex = 211.7 mV/km, Ey = 222.9 mV/km (recovery phase)
- TIE: Ex = 340 mV/km, Ey = 358.1 mV/km (main phase), Ex = 345.7 mV/km, Ey = 369.9 mV/km (recovery phase)
- KOU: Ex = 211.7 mV/km, Ey = 246.9 mV/km (main phase), Ex = 215.4 mV/km, Ey = 284.4 mV/km (recovery phase)

No consistent latitudinal pattern was observed.



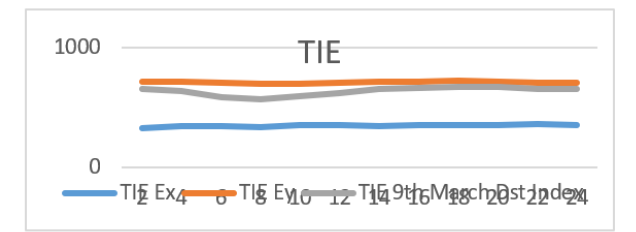


Figure 6: Geo-electric Field Responses for March 9, 1993.

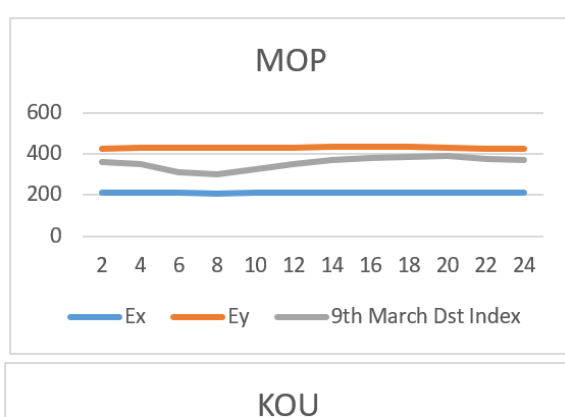
March 11, 1993

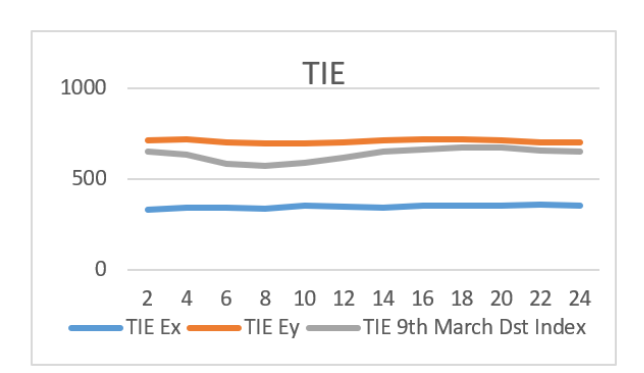
The March 11 storm showed an SSC at -44 nT around 14:00 UT: - KOU: Ex = 218.8 mV/km, Ey = 284.1 mV/km (SSC), Ex = 279.1 mV/km, Ey = 225.4 mV/km (main phase), Ex = 269.8 mV/km, Ey = 226.6 mV/km (recovery phase)

- MOP: Ex = 213.7 mV/km, Ey = 222.2 mV/km (SSC), Ex = 211.4 mV/km, Ey = 212.9 mV/km (main phase), Ex = 212.5 mV/km, Ey = 211.6 mV/km (recovery phase)
- TIE: Ex = 337.3 mV/km, Ey = 359.9 mV/km (SSC), Ex = 341.4 mV/km, Ey = 322.3 mV/km (main phase), Ex = 333.6 mV/km, Ey = 330.5 mV/km (recovery phase)

KOU showed stronger geomagnetic storm influences compared to MOP, which contrasts with observations from the February 17 and March 9 storms.

Figure 7 shows the response of the geo-electric field to 11th March 1993 storm.





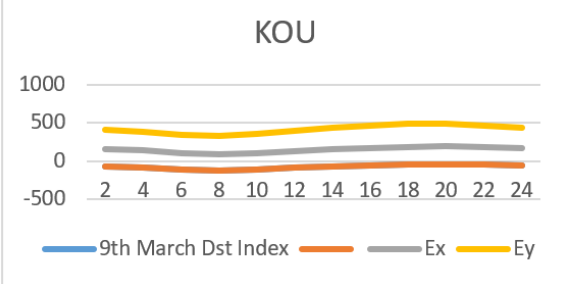


Figure 7: Geo-electric Field Responses for March 11, 1993.

April 5, 1993

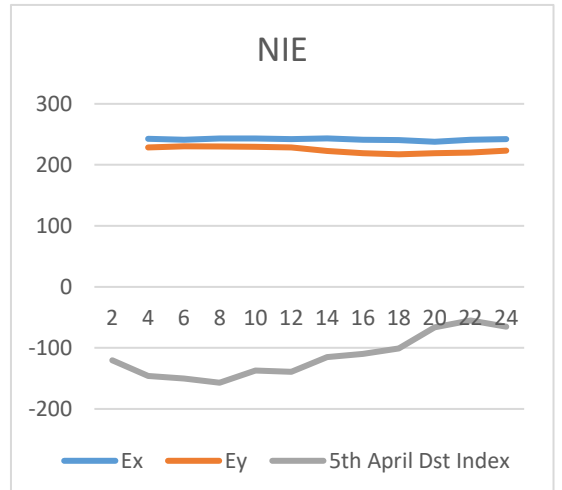
The response of geo-electric field to April 5, 1993 storm is presented in the figure 4.8

For the April 5 storm, with a Dst Index of -157 nT, no SSC was observed. Geo-electric field responses were:

- NIE: Ex = 243.2 mV/km, Ey = 230 mV/km (main phase), Ex = 242 mV/km, Ey = 228.7 mV/km (recovery phase)
- TOM: Ex = 330.4 mV/km, Ey = 347 mV/km (main phase), Ex = 330.2 mV/km, Ey = 346.6 mV/km (recovery phase)

TOM, a non-dip latitudinal station, exhibited higher amplitudes compared to NIE, with no distinct latitudinal pattern observed.

9 th MARCH 1993 CORRELATION TABLE						
FIELDS	TIE	NIE	MOP	KOU	MOP	
Н	0.417085	0.273492	0.232837	0.331526	0.274619	
Z	-0.07064	0.00761	0.180597	-0.11005	0.191864	
E_X	0.524191	-	0.043271	0.245619	0.818815	
E _Y	0.019728	-	0.053348	-	0.743939	



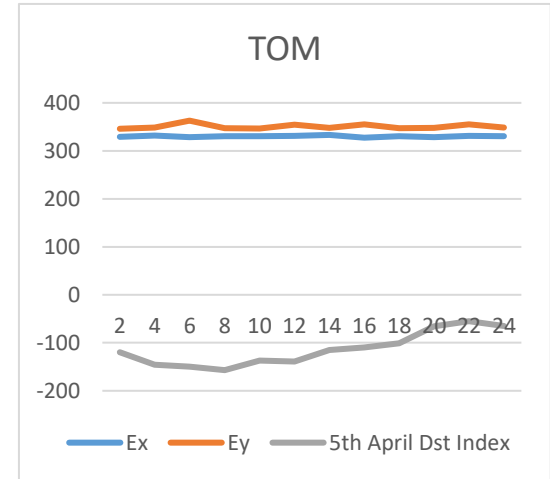


Figure 8: Geo-electric Field Responses for April 5, 1993.

17th FEB. 1993 CORRELATION TABLE						
FIELDS	TOM	LAM	MOP	NIE	SIK	
Н	0.903099	0.970954	0.975283	0.878442	0.875335	
Z	-0.18982	0.142535	-	-0.24437	-0.26644	
E_X	-0.58694	-0.25622	-0.58332	0.65873	0.023032	
E_{Y}	-0.89939	-0.32785	-0.27359	0.947974	0.243762	

3.2. CO-VARIABILITY ASSESSMENT.

The co-variability assessment of geo-electric fields, Dst Index, and geomagnetic fields was performed with the aim of evaluating the temporary relationship between the geomagnetic activity and geo-electric field responses in terms of strength, and nature of this relationships. Coefficients of correlation was determined by categorizing them as follows: 0 to 0.2 (poor), 0.3 to 0.4 (fairly poor), 0.5 to 0.6 (strong), and 0.7 to 1.0 (very strong).

Following this analysis, it was observed that the stations near the dip latitudes (KOU and NIE) exhibited varying strengths of association with the geo-electric field upon examination, indicating that storm variability does not follow a consistent pattern in latitudes. This inconsistency in pattern is said to be as a result of the differences in the materials that constitutes the location, possibly leading to differential conductivity.

Tables 3, 4, 5, and 6 present the correlation values for the storms on February 17, March 9, March 11, and April 5, 1993.

5 th APRIL 1993 CORRELATION TABLE					
FIELDS	TOM	SIK	NIE		
Н	-	0.392947	0.4212		
Z	-0.04833	-	0.095202		
E_X	-0.17264	-	-0.59566		
E _Y	-0.23643	-	0.095202		

11th MARCH 1993 CORRELATION TABLE					
FIELDS	TIE	NIE	MOP	KOU	
Н	0.361591	0.211329	0.21774	0.235585	
Z	-	-0.08426	0.008107	0.051952	
E_X	-0.17349	-	-0.00524	-0.56728	
E _Y	0.170867	-	-0.31103	-0.56728	

IV. CONCLUSION

We have investigated the Variability of geo-electric field during geomagnetic disturbances in West Africa's equatorial region.

The findings of this study are as follows:

- 1. All stations analyzed showed variations in the geo-electric field during the geomagnetic storms of February 17, 1993; March 9, 1993; March 11, 1993; and April 5, 1993 storms
- 2. These variations were seen to be more intense in stations closer to the dip equator than those farther north or south of the dip equator.
- 3. The magnitude of this variations appear to depend on local conductive materials like water on the observational location
- 4. The co-variability assessment conducted showed that geomagnetic storms and geo-electric field association depends on the differential local conductive materials of the station, hence no latitudinal pattern was observed.

REFERENCES

- [1]. Akpaneno, A., Adimula, I., & Cyril, A. (2015). Disturbed day variation of geomagnetic H-field along the magnetic equator. **Advances** in Physics Theories and Applications, 48, 7–15.
- [2]. Burns, A. G., Killeen, T. L., & Roble, R. G. (1991). A theoretical study of thermospheric composition perturbations during an impulsive geomagnetic storm. **Journal of Geophysical Research: Space Physics**, 96(A8), 14153–14167.
- [3]. Chapman, S., & Bartels, J. (1940). Geomagnetism (Vol. 2). Oxford University Press.
- [4]. Gish, O. H., & Rooney, W. J. (1930). Results of earth current observations at Huancayo Magnetic Observatory, 1927–1929. Terrestrial Magnetism and Atmospheric Electricity, 35, 213.
- [5]. Gonzalez, W. D., Joselyn, J. A., Kamide, Y., Kroehl, H. W., Rostoker, G., Tsurutani, B. T., & Vasyliunas, V. M. (1994). What is a geomagnetic storm? **Journal of Geophysical Research: Space Physics**, **99**(A4), 5771–5792.
- [6]. Hutton, R. (1962). Equatorial micropulsations and ionospheric disturbance currents. Nature, 195(4838), 269–270.
- [7]. Hutton, R., & Wright, R. W. H. (1961). Diurnal variation of earth currents at the equator. Journal of Atmospheric and Terrestrial Physics, 20, 100.
- [8]. Lakhina, G. S., & Tsurutani, B. T. (2016). Geomagnetic storms: Historical perspective to modern view. Geoscience Letters, 3(1), 5.
- [9]. Okwesili, N. A., Okeke, F. N., & Awucha, I. E. (2023). Contribution of solar quiet (Sq) daily current variations to the deep earth conductivity within the Southern African region. International Journal of Physical Sciences, 18(4), 116–128. https://doi.org/10.5897/IJPS2023.502
- [10]. Pokharia, M., Prasad, L., Bhoj, C., & Mathpal, C. (2018). Study of geomagnetic storms and solar and interplanetary parameters for solar cycles 22 and 24. Solar Physics, 293(9), 126.
- [11]. Tsurutani, B. T., & Gonzalez, W. D. (1997). The interplanetary causes of magnetic storms: A review. In B. T. Tsurutani, W. D. Gonzalez, & Y. Kamide (Eds.), **Magnetic storms** (Vol. 98, pp. 77). American Geophysical Union.